IEEE Access
Multidisciplinary | Rapid Review | Open Access Journal

Received 10 October 2024, accepted 20 November 2024, date of publication 9 December 2024,
date of current version 19 December 2024.

Digital Object Identifier 10.1109/ACCESS.2024.3512671

RESEARCH ARTICLE

Agricultural Pest Image Recognition Algorithm Based on Convolutional Neural Network and Bayesian Method

LING ZHANG[1], FAHUI WU[2], AND WENSEN YU[2]
[1]Information Technology and Laboratory Management Center, Wuyi University, Wuyishan 354300, China
[2]College of Mathematics and Computer, Wuyi University, Wuyishan 354300, China

Corresponding author: Ling Zhang (zhanglin@wuyiu.edu.cn)

This work was supported in part by the Science and Technology Innovation Joint Funding Project "Research and Application of Key Technologies for Ecological Environment Monitoring in Expressway Regions with the Integration of Heaven, Earth and Space" under Grant N2020Z016.

ABSTRACT Aiming at the limitations of existing agricultural pest image recognition technology, a novel agricultural pest recognition algorithm based on convolutional neural network and Bayesian method is proposed. During the process, convolutional neural networks are chosen as the basic model for image recognition algorithms, and Bayesian methods are used to optimize the neural network structure. At the same time, approximate variational methods are applied to construct corresponding approximate functions. Finally, the Bayesian neural network sampling optimization is completed through the method of random variable reparameterization. According to simulation experiments, the accuracy of the proposed method in classifying and recognizing beetles is 92.1%, and the accuracy in classifying and recognizing grasshoppers is 92.4%. The proposed method has an image recognition accuracy of over 90% for agricultural pests, and has the highest accuracy among the 5 image recognition methods compared. Except for the accuracy of cricket recognition, the convolutional neural network image recognition method has the lowest accuracy of agricultural pest image recognition among the five image recognition methods. The experimental results show that the proposed method can effectively recognize agricultural pest images and has good operational performance. The contribution of the research lies in proposing a novel agricultural pest image recognition algorithm and innovatively optimizing the structure of the convolutional neural network model. The Bayesian method is used to improve the estimation of weights and biases, making the model more accurate in processing agricultural pest images.

INDEX TERMS Image recognition, neural networks, Bayesian method, probability distribution, approximate function.

I. INTRODUCTION

Although the speedy advancement of agriculture has brought considerable economic benefits, it has also brought many development issues. With the expansion of agricultural production scale, the problem of agricultural pests in agricultural production has become one of the main issues limiting the development of gardens [1]. Due to the wide variety of agricultural crops, the corresponding types of agricultural pests have also increased. The complex types of pests make it difficult for non professionals to accurately identify pest types with the naked eye, and pest identification is also a time-consuming and laborious task for professionals [2]. Therefore, using manual identification of pest species can cause significant resource waste and cannot guarantee the accuracy of identification results [3]. Additionally, as targeted pest control strategies are commonly used in agricultural pest control, accurate identification of pest types is required. If the identification of pest types is incorrect, it can lead to resource waste and even serious agricultural disasters. Traditional

The associate editor coordinating the review of this manuscript and approving it for publication was Dominik Strzalka.

agricultural pest identification techniques generally use feature extraction methods to capture and classify agricultural pests in images [4]. The characteristics of agricultural pests mainly include the surface texture, morphology, size, and external organ expression of pests [5]. Due to the fact that traditional agricultural pest identification techniques mainly rely on manual feature collection, and the classification performance of recognition algorithms is average, the efficiency and accuracy of identifying agricultural pests in practical applications cannot meet the growing needs of agricultural production. With the growth of modern technology, the field of image classification algorithms is advancing rapidly, and a series of neural network structures with numerous functions have been developed. Applying neural network technology to the field of image classification and recognition can achieve good classification results. Bayesian method, as a statistical method based on Bayesian principles, can effectively solve uncertainty problems and efficiently utilize the collected raw data.

Many experts have conducted relevant research on convolutional neural networks (CNNs). Cong and Zhou raised a modular CNN architecture classification method [6]. By analyzing the advantages and disadvantages of various neural network architectures and comparing their efficacy, and based on the mathematical principles of optimization algorithms, a comprehensive classification of network compression and acceleration network architecture optimization algorithms was conducted. The experiment findings denoted that the raised method could assess the neural network architecture in specific practical applications, and quickly find the neural network algorithm that fits the problem. Xiong et al. raised a CNN algorithm with a simple door opening and closing architecture. [7] Based on liquid phase synthesis genetic information circuit for data calculation, it combined with weight sharing CNN to complete parallel multiplication and accumulation operation of 144 inputs, and a simple cyclic freeze-thaw method was used to shorten the calculation time. The experiment outcomes illustrated that the proposed algorithm could promote the development of molecular computers. Lanjewar and Gurav raised a soil image classification processing method with machine language [8]. By using a symbolic mathematics system for weight pre training, soil images were collected based on machine learning models and divided into training and validation datasets. Subsequently, the dataset was subjected to image enhancement processing and model training, followed by classification of the soil image dataset using deep CNNs. The experiment outcomes illustrated that the classification method raised by the research was superior to other traditional classification methods. Szepesi and Szilágyi proposed a novel deep neural network architecture [9]. The neural network model was trained and tested for the collected labeled images, and temporary dropout methods was utilized during the training process. The experimental results denoted that the raised network architecture had best performance in terms of accuracy, recall, and precision methods. Goyald et al. raised a face detection model based on neural networks [10]. Facial data in static and real-time videos were trained and evaluated using the Kaggle dataset. The experiment outcomes illustrated that the raised model had significant advantages in computational efficiency and accuracy, and could be used as a scanning tool for public places in practical applications.

Many scholars have conducted relevant research on Bayesian methods. Ziatdinov et al. raised a Bayesian-based deep kernel learning method [11]. Bayesian inference in data-driven methods was used as the physical foundation model and function fitting was performed, followed by structuring the high-speed process. The experiment outcomes illustrated that the raised method could be widely applied to relevant research in the field of combined imaging. Hosseini and Ivanov proposed a multi-layer Bayesian network model [12]. Based on the forward and backward propagation analysis features of Bayesian networks, the impact of different triggering factors on financial performance was simulated and evaluated. The experimental results indicated that the model proposed by the research could effectively predict the impact of the pandemic on supply chain performance. Ouyang et al. raised a Bayesian regression model [13]. A single response normal model was used as the basic model, and Bayesian techniques were combined to analyze multi feature systems, while considering high correlation, non normality, and variable selection issues. It generated posterior samples in the fully joint posterior distribution to obtain robust Bayesian estimates. Experiment outcomes illustrated that the raised model performed better than other classical models. Bartoš et al. raised a Bayesian-based publication bias adjustment method [14]. A stable Bayesian meta-analysis model was combined with a P-value selection model and an adjusted research effect model, and it weighted the impact estimates derived from competitive methods. The experiment outcomes illustrated that the raised method could optimize the adjustment of complementary publication bias. Baltussen et al. proposed a Bayesian analysis method [15]. Different network topology data was combined into a single probability analysis framework, and then new data was iteratively added to the model to improve parameter estimation and behavior prediction, while automatically considering uncertainties in the experimental process. The experiment outcomes illustrated that the raised method could promote the effectiveness of network design and generate robustness through the accumulation of experimental errors.

In summary, due to the inability of existing agricultural pest image recognition methods to accurately classify agricultural pests under external interference conditions or when there are a large number of pest species, a novel agricultural pest image recognition algorithm is proposed by combining CNNs and Bayesian methods. The CNN is used as the basic algorithm model, combined with Bayesian methods for optimization. An approximate variational method is used to construct an approximate function, and a random variable

reparameterization method is used for sampling optimization, to provide certain application value for research on agricultural pest control.

II. METHODS AND MATERIALS

A. AGRICULTURAL PEST IMAGE RECOGNITION MODEL COMBINING BAYESIAN METHOD

Due to the various drawbacks of manual recognition methods, machine learning vision technology has been broadly utilized in the field of agricultural production for image recognition of agricultural pests [16], [17]. The study selects CNN models as the main model for agricultural pest image recognition methods. CNNs can effectively solve image recognition problems [18], [19], [20]. CNN can capture local features of images through convolutional layers, which gives it a natural advantage in processing image data. In agricultural pest image recognition, local features such as texture, edges and shape are the key to recognition and classification. Moreover, the convolutional kernels in CNN share weights at multiple locations, which greatly reduces the number of model parameters, reduces the computational complexity, and improves the efficiency and generalization ability of model training. Due to the close curve shape between the Tanh function and the Sigmoid function, and the effective avoidance of zigzag phenomenon with 0 as the curve center, the study selects the Tanh function as the output layer activation function of the main model for agricultural pest image recognition, and selects the ReLu function as the hidden layer activation function. Due to the fact that the main model for agricultural pest image recognition uses CNN models, point estimation methods are mainly used for classification in the process of completing image classification and recognition tasks, which cannot effectively make trade-offs between data prediction results. Therefore, this study introduces Bayesian methods to optimize the main model for agricultural pest image recognition, transforming the neural point estimation weight method in the CNN model into a probability distribution (PD) method. Bayesian methods can predict posterior data based on collected prior data and selected representative samples, while accurately characterizing the uncertainty of the data [21], [22], [23]. The core distribution form of Bayesian method is Gaussian PD, and the Gaussian PD curve is denoted in Figure 1.

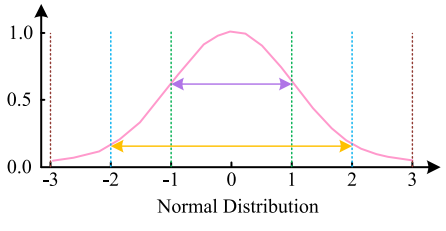

FIGURE 1. Gaussian distribution for $\mu = 0$ $\sigma = 1$.

In Figure 1, in the Gaussian distribution form of the Bayesian method, there are mainly two parameters, namely μ and σ. μ means the expected mean of the Gaussian distribution, σ means the standard deviation of the Gaussian distribution, and $\sigma 2$ means the variance. The choice of Gaussian distribution is due to its excellent mathematical properties, such as closure, differentiability, and analytic inverse function, which make it widely used in probability inference and parameter estimation. In addition, according to the central limit theorem, the sum of a large number of independent random variables tends to form a Gaussian distribution, even if the original variables do not follow a Gaussian distribution, which makes the Gaussian distribution fit the dataset. Meanwhile, Gaussian distribution has also been widely applied in practical applications, such as neural network optimization in deep learning [24]. After Gaussian distribution optimization, the parameter estimation accuracy of the network has been improved, with stronger fitting performance. In Bayesian neural networks, the weights of convolutional kernels are modeled using Gaussian distributions, which helps to better handle parameter uncertainty during training and improve the model's generalization ability [25]. The Bayesian formula in Bayesian methods can use known prior data to make probability predictions for events with correlated relationships [26]. The general expression of Bayesian formula is shown in (1).

$$P(A\,|B) = \frac{P(A)P(B\,|A)}{P(B)} \tag{1}$$

In (1), A and B represent different events, respectively; $P(A)$ represents the probability of event A occurring; $P(B)$ represents the probability of event B occurring; $P(B\,|A)$ represents the probability of event A occurring under the condition of event B. A Bayesian model is constructed based on the Bayesian formula as shown in (2).

$$\begin{cases} P(\theta\,|data) = \dfrac{P(data\,|\theta)^{*}P(\theta)}{P(data)} \\ P(\theta\,|data) \propto P(data\,|\theta)^{*}P(\theta) \end{cases} \tag{2}$$

In (2), $P(\theta)$ represents a prior distribution; $P(data)$ represents a fixed value that can be obtained from data; $P(\theta\,|data)$ represents a posterior distribution; $P(data\,|\theta)$ represents likelihood distribution. The convolutional kernel structure and CNN convolutional kernel structure corresponding to the Bayesian neural network (BNN) model constructed for agricultural pest image recognition are shown in Figure 2.

In Figure 2, after inputting the raw data in the input layer, the convolutional kernels of traditional CNNs correspond to different node neuron data, and then the output layer obtains the corresponding output results based on the convolutional kernel data. The convolutional layers of BNNs use Gaussian distribution instead of single point data in node neurons, and each convolutional kernel corresponds to different random Gaussian distribution mean and standard deviation. Since Gaussian distribution is determined by two random parameter variables, BNNs have twice the number of parameters as traditional CNNs. The weight forms of the pre-optimized CNN model and the optimized BNN model are denoted in Figure 3.

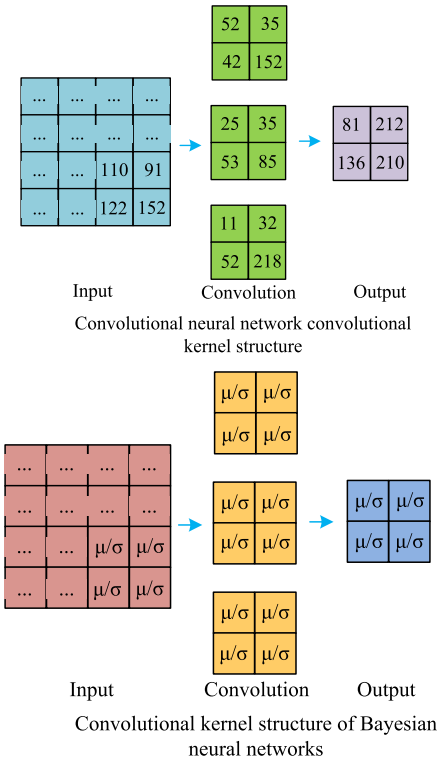

FIGURE 2. The difference of convolutional kernel structure between BNN and CNN.

In Figure 3, only the weights of individual neurons are represented. The weights between neurons in traditional CNNs have corresponding values, while in BNNs, the weights of neurons are transformed into PD mean and standard deviation forms, and the probability parameters between different neurons will obtain different numerical results after random initialization. In BNNs, uncertain parameters such as hidden layers, activation functions, and number of neurons are treated as uncertain factors or structural parameters, and the posterior probability learning corresponding to uncertain factors is treated as structural learning. The probabilistic deep learning conditional model in BNNs is shown in (3).

$$p_\theta(y\,|x) \tag{3}$$

In (3), θ means weight; x means the input data of the BNN; y represents the corresponding output value obtained after inputting x. For a single observation data, there exists a corresponding probability expression as indicated in (4).

$$p(\theta\,|D) = \frac{p(D\,|\theta)^* p(\theta)}{p(D)} \tag{4}$$

In (4), D means the observed data; θ represents the parameter; $p(\theta)$ represents the known PD of θ; $p(D)$ means the PD corresponding to the observed data; $p(D\,|\theta)$ means the likelihood PD corresponding to the observed data D. By using Bayesian inference to integrate and predict all parameters, the corresponding output data can be derived based on new input data, as expressed in (5).

$$p(y^*\,|x^*\,, D) = \int p(y^*\,|x^*\,, \theta) p(\theta\,|D) d\theta \tag{5}$$

In (5), x^* means the new input data; y^* means the output data corresponding to x^*. In BNNs, the actual PD is approximated based on an approximate PD, and samples are randomly extracted from the approximate PD to obtain a simple parameter relationship function. The function expression is shown in (6).

$$\theta^* = \arg\min_\theta \sum_{i=1}^{n} \log q_\theta(w^i\,|D) - \log p(w^{(i)}) - \log p(D\,|w^{(i)}) \tag{6}$$

In (6), q represents an approximate PD; θ^* represents the parameter relationship function; p represents the actual PD; w represents the sample data collected from an approximate PD.

B. AGRICULTURAL PEST IMAGE RECOGNITION OF IMPROVED BNN

Due to the wide variety of agricultural pests, the characteristic data corresponding to individual pest types in the dataset is scarce, and there may be too subtle differences between the characteristics of agricultural pests [27]. To avoid overfitting and improve the accuracy of pest identification, a CNN model and Bayesian method are selected to construct a BNN model. The study aims to improve the training process of BNNs by introducing a method of reparameterization of random variables. By using deterministic transformation methods to transform complex random variables in BNNs into simple random variables, the training data of BNNs can converge quickly. The schematic diagram of the improvement of random variable reparameterization is denoted in Figure 4.

In Figure 4, the use of random variable reparameterization method can ensure the sampling of distributions with parameters while preserving gradient information, thereby solving the problem of non transitive backpropagation gradients in neural network models. The fully connected layers in BNNs have been re-parameterized and improved, and the expression of weight parameters is shown in (7).

$$f(\tau) = w = \mu + \tau * \sigma, \tau \sim N(0, 1) \tag{7}$$

In (7), τ represents the sampled data corresponding to the standard Gaussian distribution. According to the weight parameter expression, the parameter update expression is obtained as shown in (8).

$$\begin{cases} \Delta\mu = \dfrac{\partial f}{\partial w} + \dfrac{\partial f}{\partial \mu} \\ \Delta\sigma = \dfrac{\partial f}{\partial w}\dfrac{\tau}{\sigma} + \dfrac{\partial f}{\partial \sigma} \\ \mu \leftarrow \mu - \alpha\Delta\mu \\ \sigma \leftarrow \sigma - \alpha\Delta\sigma \\ \theta^* = (\mu^*, \sigma^*) \end{cases} \tag{8}$$

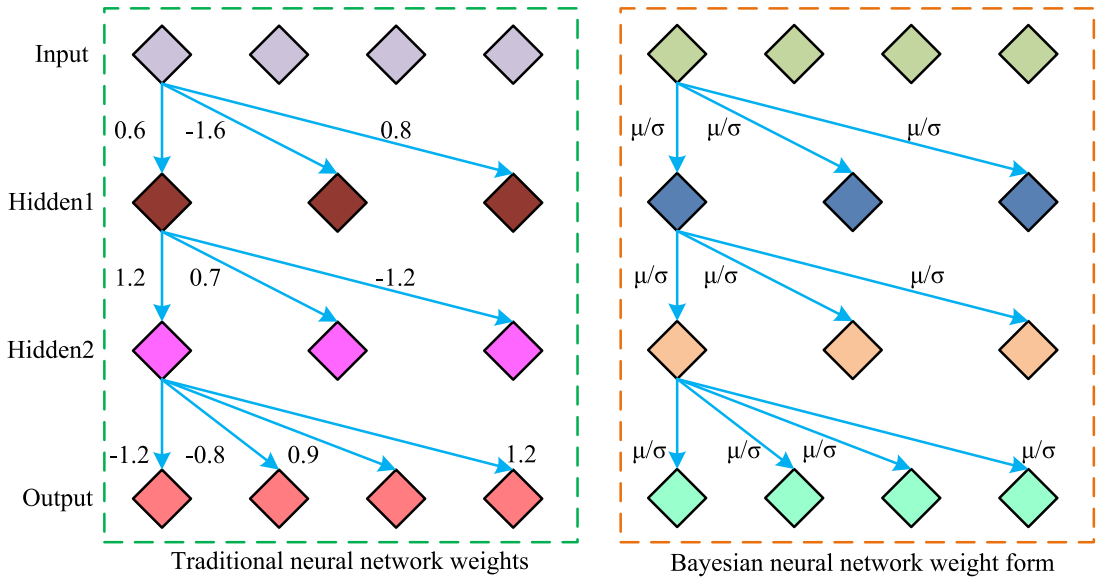

FIGURE 3. Traditional neural network weight form and BNN weight form.

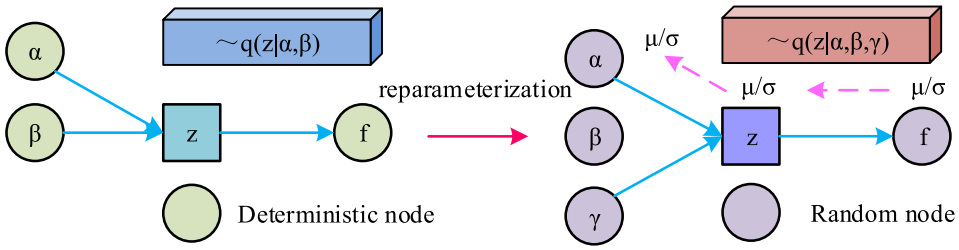

FIGURE 4. Random variable reparameterization improvement diagram.

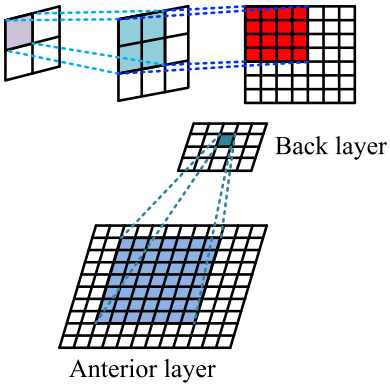

FIGURE 5. BNN receptive field structure.

In (8), α represents the proportional coefficient; $\Delta\mu$ represents the change in mean value; $\Delta\sigma$ represents the change in standard deviation. It obtains a single known weight value through sampling, and performs convolution operation on the weight value and receptive field. The receptive field structure of BNN is denoted in Figure 5.

From Figure 5, the output value of each output node in the convolutional layer of the BNN only depends on one region below the convolutional layer, and does not affect other regions of the dependent region. The expression obtained by convolution kernel convolution is shown in (9).

$$sample_{conv} = conv_{mean} + \tau conv_{std} \tag{9}$$

In (9), $sample_{conv}$ represents the convolution kernel convolution result; $conv_{mean}$ represents the mean weight distribution of the convolutional kernel; $conv_{std}$ represents the standard deviation of weight distribution. The expression for the convolution kernel and receptive field convolution result is shown in (10).

$$S = R * sample_{conv} \tag{10}$$

In (10), R represents receptive field convolution; S represents the convolution kernel and receptive field convolution results. By using convolutional results to advance the sampling process of BNNs, the forward propagation of the neural network is transformed into a differentiable form, and the weight distribution can be updated during the backpropagation process. Because BNN backpropagation mainly adjusts the parameters of weight distribution, it avoids the single point estimation defect in traditional CNN backpropagation process. However, due to the complexity of PD in BNNs,

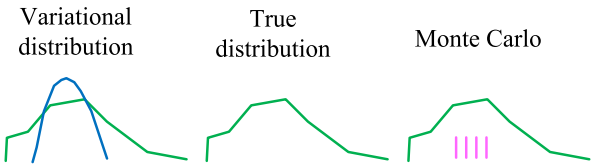

FIGURE 6. Schematic diagram of approximate probability calculation method.

it is necessary to use probability approximation calculation methods to obtain an approximate distribution function and calculate relative entropy, thereby transforming the probability approximation problem into a relative entropy solving problem. There are two main methods for approximate probability calculation, namely Monte Carlo method and variational method. The schematic diagrams of two approximate probability calculation methods are shown in Figure 6.

In Figure 6, the random sampling basis of the Monte Carlo method is based on the actual PD function, which can effectively calculate the expected probability value and generate samples based on the known PD, thereby promoting the analysis of the overall PD. The variational method essentially involves setting an approximate PD function and making it similar to the actual PD function. When setting the probability approximate distribution function, the function is generally set to a Gaussian distribution form. Variational methods approximate the true posterior distribution through optimization processes, and compared to traditional Monte Carlo methods, they typically achieve similar or better inference results at lower computational costs [28]. Moreover, the inference process transforms the approximation problem of probability distribution into a deterministic optimization problem, minimizing the difference between two probability distributions to make the inference process more stable and efficient. The study uses variational methods to transform approximate distribution functions. The Gaussian distribution expression corresponding to the minimum relative entropy value is shown in (11).

$$\theta' = \arg\min_{\theta} KL[q_\theta(w|D)\,\|p(w|D)] \tag{11}$$

In (11), KL represents relative entropy; θ' represents the Gaussian distribution parameter with the smallest relative entropy value. The expression for relative entropy divergence is shown in (12).

$$KL[q_\theta(w|D)\,\|p(w|D)] = \int q_\theta(w|D)\log\frac{q_\theta(w|D)}{p(w|D)}dw = IE_{q_\theta(w|D)}[\log\frac{q_\theta(w|D)}{p(w|D)}] \tag{12}$$

In (12), IE represents the relative entropy divergence. According to (12), it optimizes (11) to obtain the expression as shown in (13).

$$\theta' = \arg\min_{\theta} -(IE_{q_\theta(w|D)}[\log p(w|D)] - IE_{q_{\theta(w|D)}} \times [\log q_\theta(w|D)]) + \log p(D) \tag{13}$$

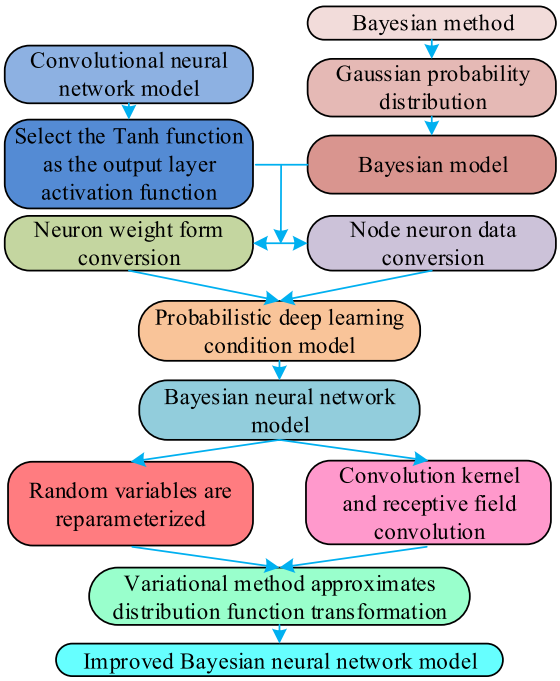

FIGURE 7. The construction process of improved BNN.

According to the optimized (13), the invariant part is decomposed and ignored, while the remaining variable part is the lower bound of the evidence. When the lower bound of evidence is maximized, the corresponding relative entropy is minimized. Therefore, the expression for the maximum logarithmic likelihood function is obtained as shown in (14).

$$\log p(D|\theta) = \beta_i KL[q_\theta(w|D)\,\|p(w|D)] + ELBO(q_\theta(w|D)) \tag{14}$$

In (14), β represents the likelihood parameter of the BNN; i represents the training data of the corresponding BNN. The likelihood function expression of BNN is shown in (15).

$$\beta_i = \frac{2^{M-i}}{2^{M-1}} \tag{15}$$

In (15), M represents the amount of sample data involved in each iteration. BNNs can solve PDs by approximating distribution functions. Finally, an improved BNN model is obtained. The research summarizes the construction process of an improved BNN model applied to agricultural pest image recognition, as shown in Figure 7.

In Figure 7, the study selects a CNN model as the basic model for agricultural pest image recognition, and selects the Tanh function as the activation function for the output layer of the CNN model. A Bayesian model expression is constructed based on the Gaussian PD in Bayesian methods. Subsequently, the CNN model is combined with Bayesian methods. During the integration process, the neuron weight form and node neuron data form in the CNN model are transformed, and a probabilistic deep learning conditional model is obtained, and then a BNN model is

TABLE 1. Simulation experiment environment configuration parameters.

Argument	Index
Operating system	Ubuntu16.04.1 64-bit
Development language and version	python3.5.2
Underlying frame	Pytorch
Graphics card configuration	TitanX
Video card memory	12GB
Call library	Pytorch
Kit	Numpy, torchvision, PIL

constructed. Subsequently, random variable reparameterization and convolution kernels and receptive field convolution are applied to the BNN model, and variational methods are used to approximate the distribution function transformation, ultimately resulting in an improved BNN model. The agricultural pest image recognition algorithm program first pre-processes the input agricultural pest image data, including image scaling, normalization, and data augmentation, to improve the robustness and generalization ability of the model. Further model construction is carried out, and the BNN model is trained using random variable reparameterization methods, including forward propagation, backward propagation, and parameter update processes. After the model training is completed, the program evaluates the test set and calculates performance indicators such as recognition accuracy, precision, and recall to verify the effectiveness of the model.

III. RESULTS

A. COMPARATIVE ANALYSIS OF PERFORMANCE SIMULATION EXPERIMENTS OF BNN MODELS

To analyze the performance of the research method, simulation experiments were set up for performance verification. The environmental configuration parameters for the simulation experiment are indicated in Table 1.

In Table 1, the operating system environment parameters for the simulation experiment were Ubuntu16.04.1 64-bit, the corresponding programming language version type of the system was Python 3.5.2, the hardware graphics card of the system used the TitanX model, and the specific memory data of the graphics card was 12GB. The tool packages involved in the simulation experiment included numpy, torchvision and PIL. To prove the effectiveness advantages of the raised BNN, a classification accuracy simulation experiment was conducted on the training process of traditional CNNs and BNNs. The comparison results of classification accuracy are shown in Figure 8.

In Figure 8, during the data training process, as the amount of iterations increased, the accuracy of neural network classification image recognition would correspondingly increase and eventually stabilize. In Figure 8 (a), the initial image recognition accuracy of the traditional CNN based on the MNIST dataset was 58.3%. It reached its highest point at 17 iterations and no longer showed significant changes with the increase of iterations. When the curve was stable, the corresponding image recognition accuracy was 96.2%.

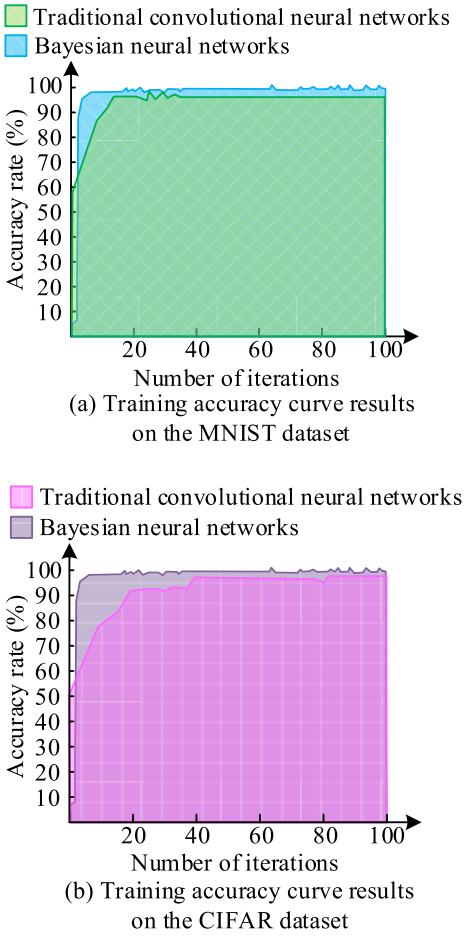

FIGURE 8. Comparison results of classification image recognition accuracy during training.

The initial image recognition accuracy of BNN was 5.4%, and after 8 iterations, the image recognition accuracy curve tended to stabilize, with a specific stable image recognition accuracy of 98.1%. In Figure 8 (b), the initial image recognition accuracy of the BNN based on the CIFAR dataset was 7.8%. After 6 iterations, the image recognition accuracy was 98.6%, and the corresponding curve trend remained stable at the same height. The initial image recognition accuracy of traditional CNNs was 51.2%. When the amount of iterations was 20, the corresponding image recognition accuracy was 92.1%. After 42 iterations, the image recognition accuracy was 94.9%. The experiment findings denoted that the initial image recognition accuracy of BNNs was low, but after iteration, it could quickly improve the image recognition accuracy. Compared with traditional CNNs, it required fewer iterations. At the same time, when the image recognition accuracy curve was stable, the corresponding accuracy was significantly higher than that of traditional CNNs. The low initial image recognition accuracy of BNNs was due to PD. Compared to traditional CNNs, BNNs had certain advantages in image recognition accuracy during dataset training.

TABLE 2. Neural network model initialization parameters based on agricultural pest image recognition.

Argument	CNN	BNNs
Loss function	Cross entropy	Lower bound of evidence
Learning rate	0.001	0.001
Batch size	10	10
λ	/	0.0005
β_i	/	$\frac{2^{M-i}}{2^{M-1}}$
Epochs	100	100
Dropout	0.5	/

B. COMPARATIVE ANALYSIS OF SIMULATION EXPERIMENTS ON IMAGE RECOGNITION OF AGRICULTURAL PESTS

The initialization parameters of the neural network model for agricultural pest image recognition are denoted in Table 2.

According to Table 2, in the initialization parameters of the neural network model for agricultural pest image recognition, the loss function in the traditional neural network model was cross entropy, and the loss function in the BNN model was the lower bound of evidence. The learning rate of both neural network models was 0.001, with the same number of iterations, with a specific value of 100. The sample size selected for each iteration was 10. The corresponding relative entropy parameter expression in BNNs was $\frac{2^{M-i}}{2^{M-1}}$, with a regularization coefficient of 0.0005. The simulation comparison results of accuracy during the training process of agricultural pest identification are shown in Figure 9.

In Figure 9, the training accuracy of deep CNNs and BNNs for agricultural pest identification increased with the amount of iterations. In Figure 9 (a), the accuracy results of the training process based on the ImageNet dataset showed that the training accuracy of the deep CNN was within the range of [1, 50] iterations, and the training accuracy improved rapidly with each iteration. Even though the training accuracy still improved within the range of [51, 100] iterations, the improvement gradually decreased, and even tended to remain unchanged. When the amount of iterations was 51, the training accuracy of the deep CNN was 72.5%, and the final stable training accuracy was 82.1%. The accuracy of BNN training was within the range of [1, 31] iterations, and the training accuracy improved rapidly with each iteration. When the amount of iterations was within the range of [32, 100], the training accuracy fluctuated slightly, and finally, the training accuracy curve remained basically unchanged as the amount of iterations increased. When the amount of iterations was 32, the training accuracy of the deep CNN was 81.5%, and the final stable training accuracy was 89.9%. In Figure 9 (b), the accuracy results of the training process based on the COCO dataset showed that the training accuracy of the deep CNN was 71.2% at 34 iterations, and 74.5% at 100 iterations. The training accuracy of BNNs was 83.4% at 33 iterations, and 92.6% at 100 iterations. The experiment outcomes indicated that the BNN model based on CNNs and Bayesian methods had significant advantages in training accuracy for image

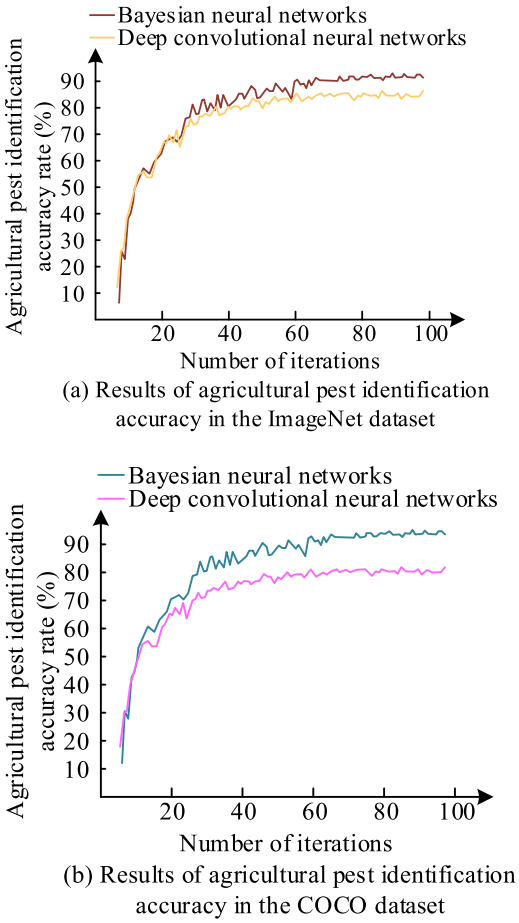

FIGURE 9. Comparison results of accuracy in the process of agricultural pest recognition training.

recognition of agricultural pests. After determining the performance advantages of BNN models in the training process of agricultural pest recognition, a comparative simulation experiment of agricultural pest image recognition was conducted based on BNNs. The comparison of classification and recognition accuracy between multi-feature fusion, support vector machine, CNN, Bayesian method, and the research proposed method for 10 types of pests is shown in Figure 10.

According to Figure 10, scarabs, grasshoppers, katydids, small gray butterflies, crickets, golden phoenix butterfly, longicorns, cicadas, poplar leaf beetles, and vegetable bugs corresponded to insect numbers 1-10, and the 10 agricultural pests were divided into two Groups A and B according to their sequence numbers. In Figure 10 (a), the accuracy rate of the proposed method in classifying and recognizing scarabs was 92.1%, the accuracy rate in classifying and recognizing grasshoppers was 92.4%, the accuracy value obtained in image recognition of katydids was 92.6%, the accuracy rate of the proposed method for small gray butterflies was 95.2%, and the accuracy rate of image recognition for crickets was 97.4%. The method proposed by the research had an image recognition accuracy of over 90% for the 5 agricultural pests

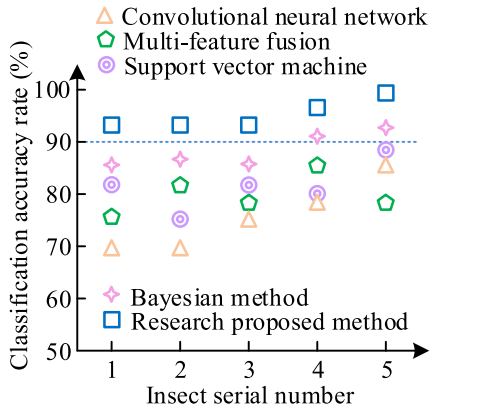

(a) Comparison of pest accuracy in group A

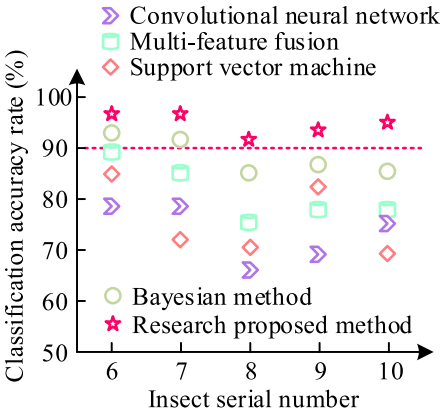

(b) Comparison of pest accuracy in group B

FIGURE 10. Comparison of accuracy rate of classification and recognition of agricultural pest images.

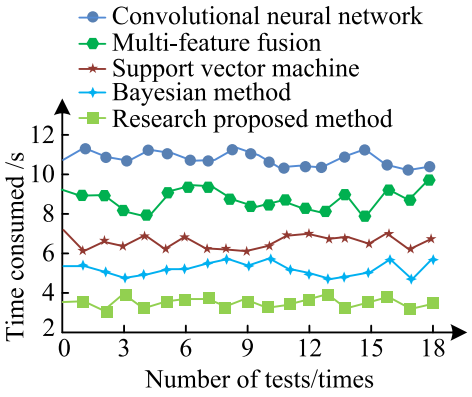

(a) Scarab image recognition

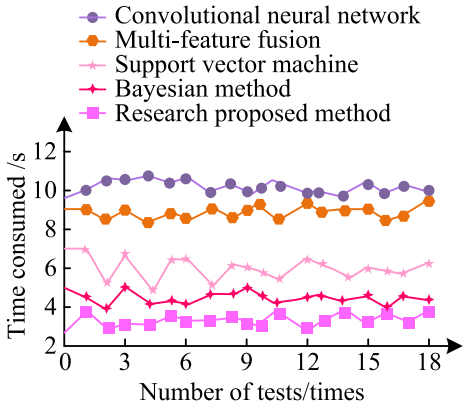

(b) Image recognition of Papilio aureus

FIGURE 11. Comparison of time consumption in agricultural pest image recognition.

in Group A, and had the highest accuracy among the 5 image recognition methods compared. Except for the accuracy of cricket recognition, the CNN image recognition method had the lowest accuracy of agricultural pest image recognition among the five image recognition methods. In Figure 10 (b), the accuracy rate of the proposed method in classifying and recognizing the golden phoenix butterfly was 96.3%, the accuracy rate in classifying and recognizing the longicorns was 97.1%, the accuracy value obtained in image recognition of the katydid was 92.6%, the accuracy rate of the proposed method corresponding to the small gray butterfly was 95.2%, and the accuracy rate of the proposed method corresponding to the cicadas was 91.7%. The method proposed by the research achieved image recognition accuracy of over 90% for the 5 agricultural pests in Group B, and the accuracy remained the highest among the 5 image recognition methods compared. Except for the accuracy of cricket recognition, the CNN image recognition method and support vector machine correspond to the lower accuracy of agricultural pest image recognition among the five image recognition methods in Group B. The experimental results indicates that the proposed method has significant advantages in the accuracy of agricultural pest image recognition. A simulation experiment was conducted on the performance advantages of the proposed method in agricultural pest image recognition in terms of time consumption. The comparison results of the experiment are shown in Figure 11.

From Figure 11, the study selected scarab and golden phoenix butterfly as the research objects. As the amount of experiments increased, the time curve of agricultural pest image recognition fluctuated up and down. In Figure 11 (a), in the recognition of beetle images, the proposed method took the least amount of time. Basically, after 3 seconds, the beetles in agricultural pest images could be correctly recognized. The consumption time curve of agricultural pests corresponding to Bayesian methods fluctuated up and down within 5 seconds, but the consumption time was not less than 4 seconds and not more than 6 seconds. CNNs consumed the most time for agricultural pest image recognition. Generally, after 11 seconds, pests belonging to the beetle category in agricultural pest images could be correctly identified. In Figure 11 (b), for the image recognition of the golden phoenix butterfly, the proposed method still consumed the least amount of time for agricultural pest image recognition, with the maximum and minimum corresponding image

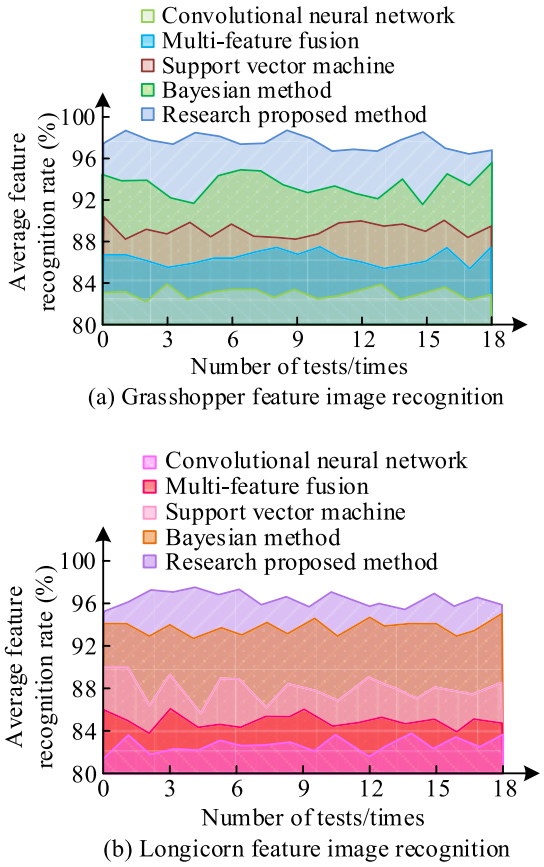

FIGURE 12. Comparison results of average recognition rate of pest characteristics.

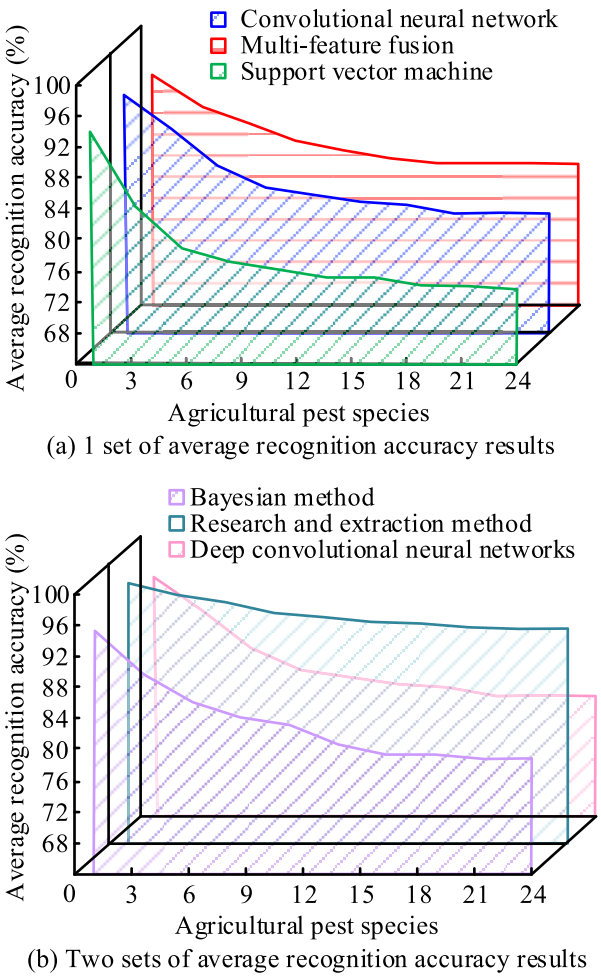

FIGURE 13. Comparison results of average recognition accuracy under different pest species.

recognition time being 3.9 seconds and 2.4 seconds, respectively. The time consumption for agricultural pest image recognition corresponding to CNNs was the highest among the five image recognition methods, with a corresponding consumption time of basically 10 seconds. The experiment findings indicated that the raised method had significant advantages in terms of time consumption for agricultural pest image recognition. A simulation experiment was completed on the average recognition rate of pest features in agricultural pest image recognition, and the experiment findings are denoted in Figure 12.

From Figure 12, the study selected grasshoppers and longhorns as the research objects. As the amount of experiments increased, the mean recognition rate curves corresponding to the five image recognition methods fluctuated up and down. In Figure 12 (a), during the image recognition process for grasshoppers, the average recognition rate of the features corresponding to the raised method fluctuated around 97.5%, while that corresponding to the CNN was the lowest, fluctuating around 83.2%. In Figure 12 (b), for the image recognition process of the beetle, the average recognition rate of the features corresponding to the Bayesian method fluctuated around 94.5%, second only to that corresponding to the raised method in the study. The experiment outcomes denoted that the raised method had outstanding performance in terms of average recognition rate of features in agricultural pest image recognition, and could effectively extract features from agricultural pest images. The comparison results of the average recognition accuracy obtained with the increase of pest types in agricultural pest image recognition are shown in Figure 13.

From Figure 13, six image recognition methods, including CNNs, multi-feature fusion, Bayesian methods, support vector machines, deep CNNs, and the proposed method, were divided into two groups. Group 1 was CNNs, multi-feature fusion, and support vector machines. Group 2 was Bayesian methods, deep CNNs, and the proposed method. As the amount of pest species increased, the average recognition accuracy corresponding to image recognition methods showed a downward trend. In Figure 13 (a), the average recognition accuracy corresponding to the CNN for identifying one agricultural pest was 95.8%, the average recognition accuracy corresponding to the support vector machine was 94.1%, and the specific value of the average recognition accuracy corresponding to multi-feature fusion was 93.9%.

TABLE 3. Comparison of other advanced technologies.

Features/Technology	Research method	AERM	ACRM
Probability inference	Correct	Deny	Deny
Feature extraction	Automatic	Automatic	Hand movement
Comprehensive accuracy rate	92.1%	85.6%	80.2%
Average response time (s)	0.85	1.20	1.51
Experimental standard deviation	2.1	3.5	4.2
Generalization ability	Strong	Medium	Medium

When performing image recognition on 24 types of pests, the average recognition accuracy corresponding to multi-feature fusion was the highest, with a specific value of 84%. In Figure 13 (b), the average recognition accuracy corresponding to the proposed method was significantly higher than other image recognition methods. When performing image recognition for one pest, the corresponding average recognition accuracy was 98.5%. When using image recognition for 24 types of agricultural pests, the corresponding average recognition accuracy was 92.6%. The experiment findings denoted that the proposed method could maintain a high average recognition accuracy while simultaneously recognizing multiple agricultural pests, and could play an important role in practical applications. In order to further analyze the superiority of the research method, the study added Algorithm of Estimation Regression Models (AERM) and Algorithm of Change Rates Matrix (ACRM) for analysis, as shown in Table 3 [29], [30].

In Table 3, the comprehensive accuracy of the research method reaches 92.1%, and it also has stronger generalization ability. The AERM method focuses on using Markov models to transform datasets and comparing actual datasets with estimated values through homogeneity tests and Mann Whitney tests, which has potential application value when dealing with samples with high dispersion. However, the AERM method requires manual operation in feature extraction, which limits its applicability in automation and large-scale data processing. The ACRM method provides a novel approach for predicting the percentage of solar radiation by constructing a rate of change matrix. Although the ACRM method performs well in solar energy prediction, its application in agricultural pest image recognition is still unclear and its accuracy is relatively low. Overall, the advantages of the research method in automated feature extraction and high accuracy make it more attractive in agricultural pest image recognition tasks.

IV. CONCLUSION

To promote the development of agricultural pest identification related technologies, this research proposed an agricultural pest identification algorithm based on CNNs and Bayesian methods. Based on the CNN model, the Bayesian method was introduced for optimization, and the optimized BNN was improved. The approximate variational method was used to construct an approximate function for the posterior PD in the BNN. At the same time, the random variable reparameterization method was used to sample and optimize the Gaussian distribution convolution kernel in the BNN, thereby solving the backpropagation problem of the BNN. According to the simulation experiment results, the initial image recognition accuracy of traditional CNNs in the MNIST dataset was 58.3%, and the highest point was basically reached at 17 iterations. When the curve was stable, the corresponding image recognition accuracy was 96.2%. The initial image recognition accuracy of BNN was 5.4%, and after 8 iterations, the image recognition accuracy curve tended to stabilize, with a specific stable image recognition accuracy of 98.1%. The accuracy of BNN training was within the range of [1, 31] iterations, and the training accuracy improved rapidly with each iteration. When the amount of iterations was within the range of [32, 100], the training accuracy fluctuated slightly, and finally, the training accuracy curve remained basically unchanged as the amount of iterations increased. The experiment findings indicate that compared to other image recognition methods, the raised method has significant performance advantages in agricultural pest image recognition, and can play a certain role in practical applications, promoting research related to agricultural pest recognition. Due to the optimization space in parameter settings during neural network training, the next step will be to conduct in-depth research on training parameter settings.

REFERENCES

[1] X. Xie, B. Xie, D. Xiong, M. Hou, J. Zuo, G. Wei, and J. Chevallier, "New theoretical ISM-K2 Bayesian network model for evaluating vaccination effectiveness," *J. Ambient Intell. Humanized Comput.*, vol. 14, no. 9, pp. 12789–12805, Jul. 2022, doi: 10.1007/s12652-022-04199-9.

[2] A. Senthil Vel, K. E. Konan, D. Cortés-Borda, and F.-X. Felpin, "Enhancing optimization of mixed variables on a robotic flow platform: Integrating statistical filtering with Nelder–Mead and Bayesian methods," *Organic Process Res. Develop.*, vol. 28, no. 5, pp. 1597–1606, May 2024, doi: 10.1021/acs.oprd.3c00238.

[3] C. M. Tribble, W. A. Freyman, M. J. Landis, J. Y. Lim, J. Barido-Sottani, B. T. Kopperud, S. Höhna, and M. R. May, "RevGadgets: An R package for visualizing Bayesian phylogenetic analyses from RevBayes," *Methods Ecology Evol.*, vol. 13, no. 2, pp. 314–323, Feb. 2022, doi: 10.1111/2041-210x.13750.

[4] Y. Yuan, L. Chen, H. Wu, and L. Li, "Advanced agricultural disease image recognition technologies: A review," *Inf. Process. Agricult.*, vol. 9, no. 1, pp. 48–59, Mar. 2022, doi: 10.1016/j.inpa.2021.01.003.

[5] H. E. Hezakiel, M. Thampi, S. Rebello, and J. M. Sheikhmoideen, "Biopesticides: A green approach towards agricultural pests," *Appl. Biochem. Biotechnol.*, vol. 196, no. 8, pp. 5533–5562, Aug. 2024, doi: 10.1007/s12010-023-04765-7.

[6] S. Cong and Y. Zhou, "A review of convolutional neural network architectures and their optimizations," *Artif. Intell. Rev.*, vol. 56, no. 3, pp. 1905–1969, Mar. 2023, doi: 10.1007/s10462-022-10213-5.

[7] X. Xiong, T. Zhu, Y. Zhu, M. Cao, J. Xiao, L. Li, F. Wang, C. Fan, and H. Pei, "Molecular convolutional neural networks with DNA regulatory circuits," *Nature Mach. Intell.*, vol. 4, no. 7, pp. 625–635, Jul. 2022, doi: 10.1038/s42256-022-00502-7.

[8] M. G. Lanjewar and O. L. Gurav, "Convolutional neural networks based classifications of soil images," *Multimedia Tools Appl.*, vol. 81, no. 7, pp. 10313–10336, Feb. 2022, doi: 10.1007/s11042-022-12200-y.

[9] P. Szepesi and L. Szilágyi, "Detection of pneumonia using convolutional neural networks and deep learning," *Biocybernetics Biomed. Eng.*, vol. 42, no. 3, pp. 1012–1022, Jul. 2022, doi: 10.1016/j.bbe.2022.08.001.

[10] H. Goyal, K. Sidana, C. Singh, A. Jain, and S. Jindal, "A real time face mask detection system using convolutional neural network," *Multimedia Tools Appl.*, vol. 81, no. 11, pp. 14999–15015, Feb. 2022, doi: 10.1007/s11042-022-12166-x.
[11] M. Ziatdinov, Y. Liu, K. Kelley, R. Vasudevan, and S. V. Kalinin, "Bayesian active learning for scanning probe microscopy: From Gaussian processes to hypothesis learning," *ACS Nano*, vol. 16, no. 9, pp. 13492–13512, Sep. 2022, doi: 10.1021/acsnano.2c05303.
[12] S. Hosseini and D. Ivanov, "A multi-layer Bayesian network method for supply chain disruption modelling in the wake of the COVID-19 pandemic," *Int. J. Prod. Res.*, vol. 60, no. 17, pp. 5258–5276, Sep. 2022, doi: 10.1080/00207543.2021.1953180.
[13] L. Ouyang, S. Zhu, K. Ye, C. Park, and M. Wang, "Robust Bayesian hierarchical modeling and inference using scale mixtures of normal distributions," *IISE Trans.*, vol. 54, no. 7, pp. 659–671, Mar. 2021, doi: 10.1080/24725854.2021.1912440.
[14] F. Bartoš, M. Maier, E. Wagenmakers, H. Doucouliagos, and T. D. Stanley, "Robust Bayesian meta-analysis: Model-averaging across complementary publication bias adjustment methods," *Res. Synth. Methods*, vol. 14, no. 1, pp. 99–116, Jan. 2023, doi: 10.1002/jrsm.1594.
[15] M. G. Baltussen, J. van de Wiel, C. L. F. Regueiro, M. Jakštaitė, and W. T. S. Huck, "A Bayesian approach to extracting kinetic information from artificial enzymatic networks," *Anal. Chem.*, vol. 94, no. 20, pp. 7311–7318, May 2022, doi: 10.1021/acs.analchem.2c00659.
[16] D. R. Sarvamangala and R. V. Kulkarni, "Convolutional neural networks in medical image understanding: A survey," *Evol. Intell.*, vol. 15, no. 1, pp. 1–22, Mar. 2022, doi: 10.1007/s12065-020-00540-3.
[17] G. Habib and S. Qureshi, "Optimization and acceleration of convolutional neural networks: A survey," *J. King Saud Univ.-Comput. Inf. Sci.*, vol. 34, no. 7, pp. 4244–4268, Jul. 2022, doi: 10.1016/j.jksuci.2020.10.004.
[18] D. Ghimire, D. Kil, and S.-H. Kim, "A survey on efficient convolutional neural networks and hardware acceleration," *Electronics*, vol. 11, no. 6, pp. 945–946, Mar. 2022, doi: 10.3390/electronics11060945.
[19] C. F. G. D. Santos and J. P. Papa, "Avoiding overfitting: A survey on regularization methods for convolutional neural networks," *ACM Comput. Surv.*, vol. 54, no. 10s, pp. 1–25, Sep. 2022, doi: 10.1145/3510413.
[20] R. Nirthika, S. Manivannan, A. Ramanan, and R. Wang, "Pooling in convolutional neural networks for medical image analysis: A survey and an empirical study," *Neural Comput. Appl.*, vol. 34, no. 7, pp. 5321–5347, Feb. 2022, doi: 10.1007/s00521-022-06953-8.
[21] J. Zhang, C. Li, Y. Yin, J. Zhang, and M. Grzegorzek, "Applications of artificial neural networks in microorganism image analysis: A comprehensive review from conventional multilayer perceptron to popular convolutional neural network and potential visual transformer," *Artif. Intell. Rev.*, vol. 56, no. 2, pp. 1013–1070, May 2022, doi: 10.1007/s10462-022-10192-7.
[22] X. Yao, X. Wang, S.-H. Wang, and Y.-D. Zhang, "A comprehensive survey on convolutional neural network in medical image analysis," *Multimedia Tools Appl.*, vol. 81, no. 29, pp. 41361–41405, Dec. 2022, doi: 10.1007/s11042-020-09634-7.
[23] M. Torres and F. Cantú, "Learning to see: Convolutional neural networks for the analysis of social science data," *Political Anal.*, vol. 30, no. 1, pp. 113–131, Jan. 2022, doi: 10.1017/pan.2021.9.
[24] J. Li, F. Ding, and T. Hayat, "A novel nonlinear optimization method for fitting a noisy Gaussian activation function," *Int. J. Adapt. Control Signal Process.*, vol. 36, no. 3, pp. 690–707, Mar. 2022, doi: 10.1002/acs.3367.
[25] R. Ravindran, M. J. Santora, and M. M. Jamali, "Camera, LiDAR, and radar sensor fusion based on Bayesian neural network (CLR-BNN)," *IEEE Sensors J.*, vol. 22, no. 7, pp. 6964–6974, Apr. 2022, doi: 10.1109/JSEN.2022.3154980.
[26] Y. Zhang, Y. Zhao, and H. Ouyang, "Stochastic model updating for assembled structures with bolted joints using a Bayesian method," *Eng. Optim.*, vol. 54, no. 11, pp. 1919–1937, Aug. 2021, doi: 10.1080/0305215x.2021.1965136.
[27] T. Chu, Z. Wang, D. Pe'er, and C. G. Danko, "Cell type and gene expression deconvolution with BayesPrism enables Bayesian integrative analysis across bulk and single-cell RNA sequencing in oncology," *Nature Cancer*, vol. 3, no. 4, pp. 505–517, Apr. 2022, doi: 10.1038/s43018-022-00356-3.
[28] M. El-Morshedy, M. S. Eliwa, and A. Tyagi, "A discrete analogue of odd Weibull-G family of distributions: Properties, classical and Bayesian estimation with applications to count data," *J. Appl. Statist.*, vol. 49, no. 11, pp. 2928–2952, Aug. 2022, doi: 10.1080/02664763.2021.1928018.
[29] M. M. El Genidy and M. S. Beheary, "Forecasting methods in various applications using algorithm of estimation regression models and converting data sets into Markov model," *Complexity*, vol. 2022, no. 1, Jan. 2022, Art. no. 2631939, doi: 10.1155/2022/2631939.
[30] M. El Genidy, W. Megahed, and K. Mahfouz, "Algorithms of solar energy prediction combined with percentile root estimation of three-parameters distributions," *Appl. Math.*, vol. 16, no. 4, pp. 529–547, Jul. 2022, doi: 10.18576/amis/160406.

LING ZHANG was born in Nanping, Fujian, in 1983. She received the bachelor's degree in computer science and technology from Fujian University of Education, in 2008, and the master's degree in software engineering from the Huazhong University of Science and Technology, in 2013, with a focus on computer applications and digital image processing technology.

Since 2009, she has been an Experimenter with Wuyi University. She has published eight academic articles, one academic work textbook, and one research project.

FAHUI WU was born in Nanping, Fujian, in 1975. He received the degree in computer science and education from Fujian Normal University, in 2000, and the master's degree in computer science and technology from Fuzhou University, in 2007, with a focus on computer graphics and computer programming.

Since 2000, he has been an Associate Professor with Wuyi University. He has published eight academic articles, one academic work textbook, and two research projects.

WENSEN YU was born in Nanping, Fujian, in 1973. He received the bachelor's degree in history education from Fujian Normal University, in 1996, the bachelor's degree in computer science and applications from Fuzhou University, in 2002, the master's degree in computer software and theory from Jiangxi Normal University, in 2004, and the Ph.D. degree in computer science and technology from Sichuan University, in 2013, with a focus on digital image processing technology.

Since 1996, he has been a Professor with Wuyi University. He has published 30 academic articles and ten research projects.